INTERNATIONAL JOURNAL OF ROBUST AND NONLINEAR CONTROL
Int. J. Robust Nonlinear Control 2016; **26**:3791–3805
Published online 7 March 2016 in Wiley Online Library (wileyonlinelibrary.com). DOI: 10.1002/rnc.3535

Robust containment control in a leader–follower network of uncertain Euler–Lagrange systems

Justin R. Klotz*,†, Teng-Hu Cheng and Warren E. Dixon

Department of Mechanical and Aerospace Engineering, University of Florida, Gainesville, FL, USA

SUMMARY

A distributed controller is developed that yields cooperative containment control of a network of autonomous dynamical systems. The networked agents are modeled with uncertain nonlinear Euler–Lagrange dynamics affected by an unknown time-varying exogenous disturbance. The developed continuous controller is robust to input disturbances and uncertain dynamics such that asymptotic convergence of the follower agents' states to the dynamic convex hull formed by the leaders' time-varying states is achieved. Simulation results are provided to demonstrate the effectiveness of the developed controller. Copyright © 2016 John Wiley & Sons, Ltd.

Received 18 September 2014; Revised 9 November 2015; Accepted 31 January 2016

KEY WORDS: nonlinear control; distributed control; robust control; containment control

1. INTRODUCTION

Cooperation of autonomous systems has been widely investigated in recent years because of its applicability to many engineering applications. Examples include the distributed control of infrastructure systems, industrial process control, vehicle formation control, and social network analysis. Instead of a single control system performing a task, multiple potentially lower-cost systems can be coordinated to achieve a network-wide goal, such as employing a team of unmanned aerial vehicles or autonomous underwater vehicles (AUVs) to perform surveillance, search and rescue, or hazardous material recollection. Consensus is a network control strategy introduced to quantify such a cooperative objective where the states of the networked systems are regulated to the same value while network neighbors simultaneously tend to each others' states during transient performance. In consensus, network interaction is commonly modeled as being distributed, where systems only use information from network neighbors to compute a control signal such that a global objective can be achieved without requiring all-to-all communication; see [1–4] for some prominent examples.

Although terminology has been inconsistent in the literature, synchronization (cf. [5–8]) typically refers to the generalization of the consensus problem by allowing the desired state of the networked systems to be time-varying. The desired trajectory for the cooperating systems is typically specified by a network leader, which can be a preset time-varying function or a physical system that the 'follower' systems interact with via sensing or communication. For example, a task that requires an expensive sensor in a search and rescue mission can be accomplished by endowing just one system with the expensive sensor and instructing the other systems to cooperatively interact with the autonomous 'leader.' This control objective is made more practical by limiting interaction with the leader to only a subset of the follower systems.

*Correspondence to: Justin R. Klotz, Department of Mechanical and Aerospace Engineering, University of Florida, Gainesville, FL 32611-6250, USA.
†E-mail: jklotz@ufl.edu

Containment control (cf. [9–18]) is a generalization of the synchronization problem that allows for a collection of leaders. Containment control is useful in applications where a team of autonomous vehicles is directed by multiple pilots or for networks of autonomous systems where only a subset of the systems is equipped with expensive sensing hardware. The typical objective in the containment control framework is to regulate the states of the networked systems to the convex hull spanned by the leaders' states, where the convex hull is used because it facilitates a convenient description of the demarcation of where the follower systems should be with respect to the leaders.

Containment control is investigated in [9] and [11] for static leaders and in [10] for a combination of static and dynamic leaders. Containment controllers for dynamic leaders and followers with linear dynamics are developed in [12–15, 19]. A controller designed for the containment of social networks with linear opinion dynamics represented with fractional order calculus is developed in [16]. Results in [17] and [18, 20] develop a model knowledge-dependent and model-free containment controller, respectively, for the case of dynamic leaders and Euler–Lagrange dynamics, where Euler–Lagrange dynamics are used for the broad applicability to many engineering systems. However, none of the previous results analyze the case where follower systems are affected by an exogenous, unknown disturbance, which has the capability of cascading and disrupting the performance of the entire network from a single source. Compared with the work in [18], the development in this work demonstrates compensation of unknown input disturbances and does not require communication of an acceleration signal from the leader or neighboring follower agents. Furthermore, whereas the stability analysis in [18] is temporally divided into an estimation segment and a subsequent Lyapunov-based stability analysis for showing network containment, which relies on the assumption of boundedness of the dynamics until estimate equivalence is reached, the present work yields asymptotic network containment throughout the entire state trajectory. A sliding-mode based controller is developed in [20] for the compensation of exogenous disturbances in containment control of an undirected network of agents with Euler–Lagrange dynamics. However, the sliding-mode portion of the controller in [20] makes the developed control law discontinuous, which is difficult to implement in practice. Compared with the development in [20], the controller developed in this paper provides compensation of unknown exogenous disturbances with a continuous control signal, which is generally much more feasible to implement. The contribution of this paper is the development of a continuous, distributed controller that provides asymptotic containment control in a network of dynamic leaders and followers with uncertain nonlinear Euler–Lagrange dynamics, despite the effects of exogenous disturbances, where at least one of the followers interacts with at least one leader and the follower network is connected. Euler–Lagrange equations of motion are used to model the agents' dynamics because of their ability to capture nonlinearities intrinsic to many engineering systems, such as robotic systems and power generators (cf. [21]), and are still the subject of active research efforts (cf. [22–24]).

2. PROBLEM FORMULATION

2.1. Preliminaries

Graph theory is used to streamline the analysis of the considered networked dynamical systems. To facilitate the subsequent analysis, consider a network of $L \in \mathbb{Z}_{>0}$ leader agents and $F \in \mathbb{Z}_{>0}$ follower agents. Communication of the follower agents is described with a fixed undirected graph, $\mathcal{G}_F = \{\mathcal{V}_F, \mathcal{E}_F\}$, where $\mathcal{V}_F \triangleq \{L+1, \ldots, L+F\}$ is the set of follower nodes and $\mathcal{E}_F \subseteq \mathcal{V}_F \times \mathcal{V}_F$ is the corresponding edge set. An undirected edge (i, j) (and also (j, i)) is an element of $\mathcal{E}_F$ if agents $i, j \in \mathcal{V}_F$ communicate information with each other; without loss of generality, the graph is considered to be simple, that is, $(i, i) \notin \mathcal{E}_F \ \forall i \in \mathcal{V}_F$. The follower agent neighbor set $\mathcal{N}_{Fi} \triangleq \{j \in \mathcal{V}_F \mid (j, i) \in \mathcal{E}_F\}$ is the set of follower agents that transmit information to agent i. The connections in $\mathcal{G}_F$ are succinctly described with the adjacency matrix $\mathcal{A}_F = \left[a_{ij}\right] \in \mathbb{R}^{F \times F}$, where $a_{ij} > 0$ if $(j, i) \in \mathcal{E}_F$ and $a_{ij} = 0$ otherwise. The Laplacian matrix $\mathcal{L}_F = \left[p_{ij}\right] \in \mathbb{R}^{F \times F}$ associated with graph $\mathcal{G}_F$ is constructed such that $p_{ii} = \sum_{j \in \mathcal{N}_{Fi}} a_{ij}$ and $p_{ij} = -a_{ij}$ if $i \neq j$. The directed graph $\mathcal{G} = \{\mathcal{V}_F \cup \mathcal{V}_L, \mathcal{E}_F \cup \mathcal{E}_L\}$ containing both the leader and follower agents is a supergraph of

DOI: 10.1002/rnc

$\mathcal{G}_F$ constructed by appending an edge $(l,i) \in \mathcal{E}_L$ to $\mathcal{G}_F$ if leader agent $l \in \mathcal{V}_L$ communicates information to follower agent $i \in \mathcal{V}_F$, where $\mathcal{V}_L \triangleq \{1,\dots,L\}$ is the leader node set and $\mathcal{E}_L \subseteq \mathcal{V}_L \times \mathcal{V}_F$ is the set of leader–follower edges. The adjacency matrix $\mathcal{A} = \left[a_{ij}\right] \in \mathbb{R}^{(L+F)\times(L+F)}$ for graph $\mathcal{G}$ is similarly defined such that $a_{ij} > 0$ if $(j,i) \in \mathcal{E}_F \cup \mathcal{E}_L$ and $a_{ij} = 0$ otherwise. Let the diagonal leader-connectivity matrix $B = \left[b_{ij}\right] \in \mathbb{R}^{F\times F}$ be defined such that $b_{ii} = \sum_{l\in\mathcal{V}_L} a_{il}$ and $b_{ij} = 0$ for $i \neq j$. The Laplacian matrix for graph $\mathcal{G}$ can be constructed similarly to $\mathcal{L}_F$ and can be represented as $\mathcal{L} = \begin{bmatrix} \mathbf{0}_{L\times L} & \mathbf{0}_{L\times F} \\ \mathcal{L}_L & \mathcal{L}_F + B \end{bmatrix}$, where $\mathcal{L}_L \in \mathbb{R}^{F\times L}$ and $\mathbf{0}$ is the zero matrix of denoted dimensions. For brevity, let the matrix $\mathcal{L}_F + B$ be abbreviated as $L_B \triangleq \mathcal{L}_F + B$.

2.2. Dynamic model and properties

The dynamics of each follower agent $i \in \mathcal{V}_F$ are described by the nonidentical Euler–Lagrange equations of motion

$$M_i(q_i)\ddot{q}_i + C_i(q_i,\dot{q}_i)\dot{q}_i + H_i(\dot{q}_i) + G_i(q_i) + d_i = \tau_i, \tag{1}$$

where $q_i \in \mathbb{R}^m$ is the generalized configuration coordinate, $M_i : \mathbb{R}^m \to \mathbb{R}^{m\times m}$ is the inertia matrix, $C_i : \mathbb{R}^m \times \mathbb{R}^m \to \mathbb{R}^{m\times m}$ is the Coriolis/centrifugal matrix, $H_i : \mathbb{R}^m \to \mathbb{R}^m$ represents friction, $G_i : \mathbb{R}^m \to \mathbb{R}^m$ represents gravitational effects, $\tau_i \in \mathbb{R}^m$ represents the vector of control inputs, and $d_i : \mathbb{R}_{\geqslant 0} \to \mathbb{R}^m$ is a time-varying nonlinear exogenous disturbance. Functional dependency will be omitted in the remainder of the paper where the meaning is clear from context. The following assumption is characteristic of physical systems with dynamics described by Euler–Lagrange equations of motion and is used to provide bounds on the effects of the inertia matrix of the dynamics of each system (cf. [11, 18, 25]).

Assumption 1
For each follower agent $i \in \mathcal{V}_F$, the inertia matrix M_i is symmetric, positive-definite, and satisfies the inequality $\underline{m}_i \|\xi\|^2 \leqslant \xi^T M_i \xi \leqslant \tilde{m}_i \|\xi\|^2 \ \forall \xi \in \mathbb{R}^m$, where $\|\cdot\|$ represents the standard Euclidean norm, $\underline{m}_i \in \mathbb{R}_{>0}$ is a known constant, and $\tilde{m}_i : \mathbb{R}^m \to \mathbb{R}_{>0}$ is a bounded function such that $\underline{m}_i \leqslant \tilde{m}_i(q_i) \leqslant \bar{m}_i \ \forall q_i \in \mathbb{R}^m$, where $\bar{m}_i \in \mathbb{R}_{>0}$ is a known constant.

The following assumptions concern the smoothness of the agents' dynamics. For example, marine craft hydrodynamics and exogenous disturbances (e.g., waves) are often modeled as smooth (cf. [26]).

Assumption 2 ([25]*)*
For each follower agent $i \in \mathcal{V}_F$, the functions M_i, C_i, H_i, G_i are second-order differentiable such that the second time derivative is bounded, provided $q_i^{(k)} \in \mathcal{L}_\infty$, $k = 0,\dots,3$.

Assumption 3 ([27]*)*
For each follower agent $i \in \mathcal{V}_F$, the time-varying disturbance term is sufficiently smooth such that it and its first two time derivatives, $d_i, \dot{d}_i, \ddot{d}_i$, are bounded by known constants.

The following assumption specifies the smoothness and boundedness of the leader trajectories. For example, in a UAV surveillance mission, the monitored area is naturally bounded.

Assumption 4
Each time-varying leader configuration coordinate, $q_l : \mathbb{R}_{\geqslant 0} \to \mathbb{R}_m$ $(l \in \mathcal{V}_L)$, is sufficiently smooth such that $q_l \in \mathcal{C}^2$; additionally, each leader configuration coordinate and its first two time derivatives are bounded such that $q_l, \dot{q}_l, \ddot{q}_l \in \mathcal{L}_\infty$.

The following assumption is necessary for the leaders' states to be able to affect the trajectories of the follower agents.

Assumption 5
For each follower agent $i \in \mathcal{V}_F$, there exists a directed path from a leader $l \in \mathcal{V}_L$ to i.

DOI: 10.1002/rnc

Note that by Assumptions 5 and [9, Lemma 4.1], the matrix L_B is positive-definite. For convenience, the follower agents' dynamics are stacked as

$$M\ddot{Q}_F + C\dot{Q}_F + H + G + d = \tau, \tag{2}$$

where

$$\begin{aligned} M &\triangleq \text{diag}\{M_{L+1}, \ldots, M_{L+F}\} \in \mathbb{R}^{Fm\times Fm} \\ Q_F &\triangleq \left[\, q_{L+1}^T, \ \ldots, \ q_{L+F}^T \,\right]^T \in \mathbb{R}^{Fm} \\ C &\triangleq \text{diag}\{C_{L+1}, \ldots, C_{L+F}\} \in \mathbb{R}^{Fm\times Fm} \\ H &\triangleq \left[\, H_{L+1}^T, \ \ldots, \ H_{L+F}^T \,\right]^T \in \mathbb{R}^{Fm} \\ G &\triangleq \left[\, G_{L+1}^T, \ \ldots, \ G_{L+F}^T \,\right]^T \in \mathbb{R}^{Fm} \\ d &\triangleq \left[\, d_{L+1}^T, \ \ldots, \ d_{L+F}^T \,\right]^T \in \mathbb{R}^{Fm} \\ \tau &\triangleq \left[\, \tau_{L+1}^T, \ \ldots, \ \tau_{L+F}^T \,\right]^T \in \mathbb{R}^{Fm}. \end{aligned}$$

3. CONTROL OBJECTIVE

The objective is to design a continuous controller for the follower agent dynamics in (1) that drives the states of all follower agents to the (possibly time-varying) convex hull spanned by the leader agents' states despite exogenous nonlinear input disturbances and modeling uncertainties. Furthermore, only the configuration coordinate and its first time derivative are assumed to be measurable for the leader and follower agents. An error signal, $e_{1,i} \in \mathbb{R}^m$ $(i \in \mathcal{V}_F)$, is developed to quantify the neighborhood tracking error as

$$e_{1,i} \triangleq \sum_{j\in\mathcal{V}_F\cup\mathcal{V}_L} a_{ij}\left(q_i - q_j\right), \tag{3}$$

which includes the state difference between neighboring follower agents and neighboring leader agents. Note that there is no restriction on an edge weight a_{ij} for an existing connection $(i, j) \in \mathcal{E}$ other than the weight is positive and $a_{ij} = a_{ji}$ $\forall i, j \in \mathcal{V}_F$. Therefore, the control can emphasize a connection (j, i) by increasing a_{ij} if it is desired for agent $i \in \mathcal{V}_F$ to maintain close similarity to agent $j \in \mathcal{V}_F \cup \mathcal{V}_L$. An auxiliary tracking error, $e_{2,i} \in \mathbb{R}^m$, is designed as

$$e_{2,i} \triangleq \dot{e}_{1,i} + \alpha_{1,i} e_{1,i},$$

where $\alpha_{1,i} \in \mathbb{R}_{>0}$ is a constant gain. By stacking the follower agents' error signals $e_{1,i}$ and $e_{2,i}$ as $E_1 \triangleq \left[e_{1,L+1}^T, \ldots, e_{1,L+F}^T\right]^T \in \mathbb{R}^{Fm}$ and $E_2 \triangleq \left[e_{2,L+1}^T, \ldots, e_{2,L+F}^T\right]^T \in \mathbb{R}^{Fm}$, the network error dynamics can be written as

$$E_1 = (L_B \otimes I_m)\, Q_F + (\mathcal{L}_L \otimes I_m)\, Q_L, \tag{4}$$

$$E_2 = \dot{E}_1 + \Lambda_1 E_1, \tag{5}$$

where $\otimes$ represents the Kronecker product, I is the identity matrix of denoted dimensions, $Q_L \triangleq \left[\, q_1^T, \ \ldots, \ q_L^T \,\right]^T \in \mathbb{R}^{Lm}$ is the stack of leader agent states, and $\Lambda_1 \triangleq \text{diag}\{\alpha_{1,L+1}, \ldots, \alpha_{1,L+F}\} \otimes I_m \in \mathbb{R}^{Fm\times Fm}$ is a diagonal matrix of gains. An auxiliary error signal, $R \in \mathbb{R}^{Fm}$, is designed as

$$R \triangleq (L_B \otimes I_m)^{-1}\left(\dot{E}_2 + \Lambda_2 E_2\right), \tag{6}$$

DOI: 10.1002/rnc

where the matrix $L_B \otimes I_m$ is invertible because L_B is invertible and $\Lambda_2 \triangleq \text{diag}\{\alpha_{2,L+1}, \ldots, \alpha_{2,L+F}\} \otimes I_m \in \mathbb{R}^{Fm \times Fm}$ is a diagonal matrix containing the gains $\alpha_{2,i} \in \mathbb{R}_{>0}$. The auxiliary error signal R is not used in the subsequently designed controller because it depends on the second derivative of the configuration coordinate and is only introduced to facilitate an expression for the closed-loop error system.

Similar to [15], the error system in (3) is designed such that $\|E_1\| \to 0$ implies that the Euclidean distance from q_i to the convex hull formed by the leader agents also asymptotically converges to zero for all $i \in \mathcal{V}_F$. This implication is stated in the following lemma, which is used in the subsequent development.

Lemma 1
If Assumption 5 is satisfied, then $\|E_1\| \to 0$ implies that $\mathrm{d}(q_i, \text{Conv}\{q_l \mid l \in \mathcal{V}_L\}) \to 0 \ \forall i \in \mathcal{V}_F$, where $\text{Conv}\{\cdot\}$ denotes the convex hull of the set of points in its argument and the distance $\mathrm{d}(p, S)$ between a point p and a set S is defined as $\inf_{s \in S} \|p - s\|$ for all $p \in \mathbb{R}^n$ and $S \subset \mathbb{R}^n$.

Proof
See the Appendix. □

4. CONTROLLER DEVELOPMENT

An open-loop error system is designed by pre-multiplying the auxiliary tracking error R in (6) by M and using (2), (4), and (5) as

$$MR = \tau - d + S_1 + S_2, \tag{7}$$

where the functions $S_1 \in \mathbb{R}^{Fm}$ and $S_2 \in \mathbb{R}^{Fm}$ are defined as

$$\begin{aligned} S_1 \triangleq & M(Q_F)(L_B \otimes I_m)^{-1}\left((\Lambda_1 + \Lambda_2)E_2 - \Lambda_1^2 E_1\right) - C\left(Q_F, \dot{Q}_F\right)\dot{Q}_F - H\left(\dot{Q}_F\right) - G(Q_F) \\ & + M(Q_F)\left(L_B^{-1}\mathcal{L}_L \otimes I_m\right)\ddot{Q}_L + H\left(\left(L_B^{-1}\mathcal{L}_L\right) \otimes I_m\right)\dot{Q}_L\right) + G\left(\left(\left(L_B^{-1}\mathcal{L}_L\right) \otimes I_m\right)Q_L\right) \\ & + C\left(\left(\left(L_B^{-1}\mathcal{L}_L\right) \otimes I_m\right)Q_L, \left(\left(L_B^{-1}\mathcal{L}_L\right) \otimes I_m\right)\dot{Q}_L\right)\left(\left(L_B^{-1}\mathcal{L}_L\right) \otimes I_m\right)\dot{Q}_L \\ & - M\left(\left(\left(L_B^{-1}\mathcal{L}_L\right) \otimes I_m\right)Q_L\right)\left(L_B^{-1}\mathcal{L}_L \otimes I_m\right)\ddot{Q}_L, \end{aligned}$$

$$\begin{aligned} S_2 \triangleq & -C\left(\left(\left(L_B^{-1}\mathcal{L}_L\right) \otimes I_m\right)Q_L, \left(\left(L_B^{-1}\mathcal{L}_L\right) \otimes I_m\right)\dot{Q}_L\right) \\ & \times \left(\left(L_B^{-1}\mathcal{L}_L\right) \otimes I_m\right)\dot{Q}_L - H\left(\left(\left(L_B^{-1}\mathcal{L}_L\right) \otimes I_m\right)\dot{Q}_L\right) \\ & - G\left(\left(\left(L_B^{-1}\mathcal{L}_L\right) \otimes I_m\right)Q_L\right) + M\left(\left(\left(L_B^{-1}\mathcal{L}_L\right) \otimes I_m\right)Q_L\right)\left(L_B^{-1}\mathcal{L}_L \otimes I_m\right)\ddot{Q}_L. \end{aligned}$$

Terms in (7) are organized so that, after a mean value theorem-based approach (cf. [28, Lemma 5]), $\|S_1\|$ can be upper-bounded by a function of the errors signals E_1, E_2, R and $\|S_2\|$ can be upper-bounded by a constant. Note that the term $M(Q_F)(L_B \otimes I_m)^{-1}\left((\Lambda_1 + \Lambda_2)E_2 - \Lambda_1^2 E_1\right)$ can be upper-bounded by a function of the error signals using a mean value theorem-based approach after adding and subtracting the term $M\left(\left(\left(L_B^{-1}\mathcal{L}_L\right) \otimes I_m\right)Q_L\right)(L_B \otimes I_m)^{-1} \times \left((\Lambda_1 + \Lambda_2)E_2 - \Lambda_1^2 E_1\right)$ within S_1.

The developed robust distributed controller for follower agent $i \in \mathcal{V}_F$ is designed as

$$\tau_i = \sum_{j \in \mathcal{N}_{Fi}} a_{ij}\left(\left(k_{s,j} + I_m\right)e_{2,j} - \left(k_{s,i} + I_m\right)e_{2,i}\right) - b_{ii}\left(k_{s,i} + I_m\right)e_{2,i} + \nu_i, \tag{8}$$

where the function[‡] $\nu_i : \Pi_{j=1}^{|\mathcal{N}_{Fi}|+1}\mathbb{R}^m \to \mathbb{R}^m$ is the generalized solution to the differential equation

[‡]In this context, Π denotes the Cartesian product.

DOI: 10.1002/rnc

$$\dot{\nu}_i \triangleq \sum_{j\in\mathcal{N}_{Fi}} a_{ij}\left(\left(k_{s,j}+I_m\right)\alpha_{2,j}e_{2,j}-\left(k_{s,i}+I_m\right)\alpha_{2,i}e_{2,i}\right) + \sum_{j\in\mathcal{N}_{Fi}} a_{ij}\left(\chi_j \mathrm{Sgn}\left(e_{2,j}\right)-\chi_i \mathrm{Sgn}\left(e_{2,i}\right)\right)-\left(k_{s,i}+I_m\right)b_{ii}\alpha_{2,i}e_{2,i}-b_{ii}\chi_i \mathrm{Sgn}\left(e_{2,i}\right) \tag{9}$$

with $\nu_i(0) = \nu_{i0} \in \mathbb{R}^m$ as a user-specified initial condition, where $k_{s,i} \in \mathbb{R}^{m\times m}$ is a constant positive-definite gain matrix, $\chi_i \in \mathbb{R}^{m\times m}$ is a constant diagonal positive-definite gain matrix, the function $\mathrm{Sgn}(\cdot)$ is defined for all $\xi = \left[\xi_1, \ldots, \xi_v\right]^T \in \mathbb{R}^v$ as $\mathrm{Sgn}(\xi) \triangleq \left[\mathrm{sgn}\left(\xi_1\right), \ldots, \mathrm{sgn}\left(\xi_v\right)\right]^T$, and $|\cdot|$ denotes set cardinality for a set argument. Note that the controller in (8) is continuous, only relies on the configuration coordinate and its first derivative, and is distributed in communication: agent i requires its own error signal and the error signals of neighbors $j \in \mathcal{N}_{Fi}$. The use of neighbors' error signals in the control law provides cooperation among the follower agents. Assuming that a neighbor's state can be sensed, then only one-hop communication is necessary to compute the control authority in (8). In (8) and (9), the terms multiplied by the gain $k_{s,i}$ provide proportional and derivative feedback and the signum-based terms multiplied by the gain χ_i provide robust feedback that is used to reject the unknown time-varying disturbances, as shown in the following stability analysis. Similar to how sliding-mode-based controllers use the signum function to compensate for exogenous disturbances, the developed approach uses the signum function in the derivative of the controller to compensate for exogenous disturbances, provided that they are sufficiently smooth (Assumption 3). Note that a strategy involving additive gradient-based control terms, such as that in [29], can be used if collision avoidance is necessary for the control objective.

After taking the time-derivative of (7), the closed-loop error system is

$$M\dot{R} = -\left(L_B\otimes I_m\right)\left(K_s+I_{Fm}\right)\left(\dot{E}_2+\Lambda_2 E_2\right)-\left(L_B\otimes I_m\right)\beta \mathrm{Sgn}\left(E_2\right)+\tilde{N}+\left(L_B\otimes I_m\right)N_d - \left(L_B\otimes I_m\right)E_2-\frac{1}{2}\dot{M}R, \tag{10}$$

where the first two terms are contributions from the derivative of the stack of follower agents' control inputs $\dot{\tau} = \left(L_B\otimes I_m\right)\left(K_s+I_{Fm}\right)\left(\dot{E}_2+\Lambda_2 E_2\right)-\left(L_B\otimes I_m\right)\beta \mathrm{Sgn}\left(E_2\right)$; $K_s \triangleq \mathrm{diag}\left(k_{s,L+1},\ldots,k_{s,L+F}\right) \in \mathbb{R}^{Fm\times Fm}$ is a block-diagonal gain matrix and $\beta \triangleq \mathrm{diag}\left(\chi_{L+1},\ldots,\chi_{L+F}\right) \in \mathbb{R}^{Fm\times Fm}$ is a diagonal gain matrix; and the unknown auxiliary functions $\tilde{N} : \Pi_{j=1}^{7}\mathbb{R}^{Fm} \to \mathbb{R}^{Fm}$ and $N_d : \mathbb{R}_{\geqslant 0} \to \mathbb{R}^{Fm}$ are defined as

$$\tilde{N} \triangleq \dot{S}_1+\left(L_B\otimes I_m\right)E_2-\frac{1}{2}\dot{M}R, \tag{11}$$

$$N_d \triangleq \left(L_B^{-1}\otimes I_m\right)\left(\dot{d}+\dot{S}_2\right). \tag{12}$$

Terms in $\tilde{N}$ are segregated such that after taking advantage of the expressions $Q_F = \left(L_B^{-1}\otimes I_m\right)E_1-\left(L_B^{-1}\otimes I_m\right)\left(\mathcal{L}_L\otimes I_m\right)Q_L$, $\dot{E}_1 = E_2-\Lambda_1 E_1$, and $\dot{E}_2 = \left(L_B\otimes I_m\right)R-\Lambda_2 E_2$, Assumptions 2 and 4, and a mean value theorem-based approach (cf. [28, Lemma 5]), (11) can be upper-bounded by

$$\left\|\tilde{N}\right\| \leqslant \rho\left(\|Z\|\right)\|Z\|, \tag{13}$$

where $Z \in \mathbb{R}^{3Fm}$ is the composite error vector defined as $Z \triangleq \left[E_1^T \;\; E_2^T \;\; R^T\right]^T$ and $\rho : \mathbb{R}_{\geqslant 0} \to \mathbb{R}_{\geqslant 0}$ is a strictly increasing, radially unbounded function. Moreover, other terms in (10) are segregated in the function N_d such that it and its first derivative can be upper-bounded such that, for all $k \in \{1,\ldots,Fm\}$,

$$\sup_{t\in[0,\infty)} |N_d|_k \leqslant \delta_{a,k},$$

DOI: 10.1002/rnc

$$\sup_{t\in[0,\infty)} \left|\dot{N}_d\right|_k \leq \delta_{b,k},$$

after using Assumptions 3 and 4, where $|\cdot|_k$ denotes the absolute value of the k^{th} component of the vector argument and $\delta_{a,k}, \delta_{b,k} \in \mathbb{R}_{>0}$ are constant bounds. In the subsequent stability analysis, the terms in N_d and $\dot{N}_d$ are compensated by using the signum feedback terms in (9). For clarity in the following section, let the vectors $\Delta_{a,i}, \Delta_{b,i} \in \mathbb{R}^m$ be defined such that $\Delta_{a,i} \triangleq \left[\begin{array}{ccc} \delta_{a,m(i-1)+1} & \cdots & \delta_{a,m(i-1)+m} \end{array}\right]^T$ and $\Delta_{b,i} \triangleq \left[\begin{array}{ccc} \delta_{b,m(i-1)+1} & \cdots & \delta_{b,m(i-1)+m} \end{array}\right]^T$, which represent the contribution of the disturbance terms for each agent.

5. STABILITY ANALYSIS

An auxiliary function $P : \mathbb{R}^{Fm} \times \mathbb{R}^{Fm} \times \mathbb{R}_{\geq 0} \to \mathbb{R}$ is included in the subsequently defined candidate Lyapunov function so that sufficient gain conditions may be obtained for the compensation of the bounded disturbance terms in N_d. Let P be defined as the generalized solution to the differential equation

$$\begin{aligned} \dot{P} &= -\left(\dot{E}_2 + \Lambda_2 E_2\right)^T \left(N_d - \beta \operatorname{Sgn}\left(E_2\right)\right), \\ P(0) &= \sum_{k=1}^{Fm} \beta_{k,k} \left|E_2(0)\right|_k - E_2^T(0) N_d(0), \end{aligned} \tag{14}$$

where $\beta_{k,k}$ denotes the k^{th} diagonal entry of the diagonal gain matrix β. Provided the sufficient gain condition in (18) is satisfied, then $P \geq 0$ for all $t \in [0, \infty)$ [8].

Remark 1

Because the closed-loop error system in (10) and the derivative of the signal P in (14) are discontinuous, the existence of Filippov solutions in the given differential equations is addressed before the Lyapunov-based stability analysis is presented. Consider the composite vector $\eta \triangleq \left[\begin{array}{ccccc} Z^T & v_{L+1}^T & \cdots & v_{L+F}^T & \sqrt{P} \end{array}\right]^T \in \mathbb{R}^{4Fm+1}$, composed of the stacked error signals, the signal contributing discontinuities to the derivative of the developed controller, and the aforementioned auxiliary signal P. Existence of Filippov solutions for the closed-loop dynamical system $\dot{\eta} = \mathcal{K}[h_1](\eta, t)$ can be established, where $h_1 : \mathbb{R}^{4Fm+1} \times \mathbb{R}_{\geq 0} \to \mathbb{R}^{4Fm+1}$ is a function defined as the right-hand side of $\dot{\eta}$ and $\mathcal{K}[h_1](\varrho, t) \triangleq \cap_{\delta>0} \cap_{\mu(S_m)=0} \overline{\text{co}}\, h_1\left(B_\delta(\varrho) \setminus S_m, t\right)$, where $\delta \in \mathbb{R}$, $\cap_{\mu(S_m)=0}$ denotes the intersection over the sets S_m of Lebesgue measure zero, $\overline{\text{co}}$ denotes convex closure, and $B_\delta(\varrho) \triangleq \left\{\sigma \in \mathbb{R}^{4Fm+1} \mid \|\varrho - \sigma\| < \delta\right\}$, where $\sigma, \varrho \in \mathbb{R}^{4Fm+1}$ are used as dummy variables [30–32].

Let the auxiliary gain constant $\Phi \in \mathbb{R}$ be defined as

$$\Phi \triangleq \min\left\{\min_{i\in\mathcal{V}_F} \alpha_{1,i} - \frac{1}{2}, \min_{i\in\mathcal{V}_F} \alpha_{2,i} - \frac{1}{2}, \lambda_{\min}\left(L_B^2\right)\right\},$$

where $\lambda_{\min}(\cdot)$ denotes the minimum eigenvalue. A continuously differentiable, positive-definite candidate Lyapunov function $V_L : \mathcal{D} \to \mathbb{R}$ is defined as

$$V_L(y, t) \triangleq \frac{1}{2} E_1^T E_1 + \frac{1}{2} E_2^T E_2 + \frac{1}{2} R^T M(t) R + P, \tag{15}$$

where the composite vector $y \in \mathbb{R}^{3Fm+1}$ is defined as $y \triangleq \left[\begin{array}{cc} Z^T & \sqrt{P} \end{array}\right]^T$, $\mathcal{D}$ is defined as the open and connected set

$$\mathcal{D} \triangleq \left\{\sigma \in \mathbb{R}^{3Fm+1} \mid \|\sigma\| < \inf\left(\rho^{-1}\left\{\left(\left[2\sqrt{\Phi \lambda_{\min}\left(\left(L_B \otimes I_m\right) K_s \left(L_B \otimes I_m\right)\right)}\right), \infty\right)\right\}\right)\right\},$$

DOI: 10.1002/rnc

and $\rho^{-1}\{\cdot\}$ denotes the inverse mapping of a set argument. To facilitate the description of the semi-global property of the following Lyapunov-based stability analysis, the set of stabilizing initial conditions $\mathcal{S}_{\mathcal{D}} \subset \mathcal{D}$ is defined as

$$\mathcal{S}_{\mathcal{D}} \triangleq \left\{\sigma \in \mathcal{D} \mid \|\sigma\| < \sqrt{\frac{\lambda_1}{\lambda_2}} \inf\left(\rho^{-1}\left\{\left(\left[2\sqrt{\Phi\lambda_{\min}\left(\left(L_B \otimes I_m\right) K_s \left(L_B \otimes I_m\right)\right)}\right), \infty\right)\right\}\right)\right\}.$$

Because of the construction of V_L in (15), V_L satisfies the inequalities

$$\lambda_1 \|y\|^2 \leqslant V_L(y,t) \leqslant \lambda_2 \|y\|^2 \ \forall t \in [0,\infty), \tag{16}$$

where $\lambda_1, \lambda_2 \in \mathbb{R}_{>0}$ are constants defined as $\lambda_1 \triangleq \frac{1}{2}\min\left\{1, \min_{j\in\mathcal{V}_F} \underline{m}_j\right\}$ and $\lambda_2 \triangleq \max\left\{1, \frac{1}{2}\max_{j\in\mathcal{V}_F} \bar{m}_j\right\}$ via Assumption 1. The following theorem describes the performance of the networked dynamical systems through the use of the Lyapunov function candidate in (15).

Theorem 1

For every follower agent $i \in \mathcal{V}_F$, the distributed controller in (8) guarantees that all signals are bounded under closed-loop control and that containment control is semi-globally achieved in the sense that $\mathrm{d}\left(q_i, \mathrm{Conv}\left\{q_l \mid l \in \mathcal{V}_L\right\}\right) \to 0$ as $t \to \infty$, provided that the gains $k_{s,i}$, for all $i \in \mathcal{V}_F$, are selected sufficiently large such that the initial condition $y(0)$ lies within the set of stabilizing initial conditions $\mathcal{S}_{\mathcal{D}}$, and the gains $\alpha_{1,i}, \alpha_{2,i}, \chi_i$ are selected according to the sufficient conditions

$$\alpha_{1,i} > \frac{1}{2}, \quad \alpha_{2,i} > \frac{1}{2}, \tag{17}$$

$$\lambda_{\min}(\chi_i) > \|\Delta_{a,i}\|_\infty + \frac{1}{\alpha_{2,i}} \|\Delta_{b,i}\|_\infty \tag{18}$$

for all $i \in \mathcal{V}_F$, where $\|\cdot\|_\infty$ denotes the infinity norm.

Proof

Using Filippov's framework, a Filippov solution can be established for the closed-loop system $\dot{y} = h_2(y,t)$, where $h_2 : \mathbb{R}^{3Fm+1} \times \mathbb{R}_{\geqslant 0} \to \mathbb{R}^{3Fm+1}$ denotes the right-hand side of the derivative of the closed-loop error signals and $\dot{P}$. Accordingly, the time derivative of (15) exists almost everywhere $(a.e.)$ on the time domain $[0,\infty)$ and $\dot{V}_L \overset{a.e.}{\in} \dot{\tilde{V}}_L$, where

$$\dot{\tilde{V}}_L = \cap_{\xi\in\partial V_L(y,t)} \xi^T \mathcal{K}\left[\begin{array}{cccc} \dot{E}_1^T & \dot{E}_2^T & \dot{R}^T & \frac{1}{2}P^{-\frac{1}{2}}\dot{P} \ 1 \end{array}\right]^T, \tag{19}$$

where ∂V_L is the generalized gradient of V_L and the entry 1 in (19) accommodates for the expression of M as time-dependent in (15). Because $V_L(y,t)$ is continuously differentiable,

$$\dot{\tilde{V}}_L \subseteq \nabla V_L \mathcal{K}\left[\begin{array}{cccc} \dot{E}_1^T & \dot{E}_2^T & \dot{R}^T & \frac{1}{2}P^{-\frac{1}{2}}\dot{P} \ 1 \end{array}\right]^T, \tag{20}$$

where $\nabla V_L \triangleq \left[\begin{array}{cccc} E_1^T & E_2^T & R^T M & 2P^{\frac{1}{2}} \ \frac{1}{2}R^T\dot{M}(t)R \end{array}\right]$. After using the calculus for $\mathcal{K}[\cdot]$ from [30] and substituting expressions from (5), (6), (10) and (14), (20) may be written as

$$\begin{aligned}\dot{\tilde{V}}_L \subseteq & E_1^T\left(E_2 - \Lambda_1 E_1\right) + E_2^T\left(\left(L_B \otimes I_m\right) R - \Lambda_2 E_2\right) \\ & + R^T\Big(-\left(L_B \otimes I_m\right)\left(K_s + I_{Fm}\right)\left(\dot{E}_2 + \Lambda_2 E_2\right) - \left(L_B \otimes I_m\right)\beta\mathcal{K}\left[\mathrm{Sgn}\left(E_2\right)\right] + \tilde{N} + L_B N_d \\ & - \left(L_B \otimes I_m\right) E_2 - \frac{1}{2}\dot{M} R\Big) + \frac{1}{2}R^T\dot{M}R - \left(\dot{E}_2 + \Lambda_2 E_2\right)^T\left(N_d - \beta\mathcal{K}\left[\mathrm{Sgn}\left(E_2\right)\right]\right),\end{aligned} \tag{21}$$

DOI: 10.1002/rnc

where $\mathcal{K}[\mathrm{Sgn}(E_2)]_k = 1$ if $E_{2_k} > 0$, $\mathcal{K}[\mathrm{Sgn}(E_2)]_k = -1$ if $E_{2_k} < 0$, $\mathcal{K}[\mathrm{Sgn}(E_2)]_k \in [-1, 1]$ if $E_{2_k} = 0$, and here the subscript k denotes the k^{th} vector entry [30]. The set in (21) reduces to a scalar because the right-hand side is continuous $a.e.$ because of the structure of the error signals; that is, the right-hand side is continuous except for the Lebesgue negligible set of time instances in which $R^T (L_B \otimes I_m) \beta \mathcal{K}[\mathrm{Sgn}(E_2)] - R^T (L_B \otimes I_m) \beta \mathcal{K}[\mathrm{Sgn}(E_2)] \neq \{0\}$[§]. After canceling common terms, using the Raleigh–Ritz theorem and triangle inequality, recalling that L_B is positive-definite and symmetric, and using the bounding strategy in (13), the scalar value $\dot{V}_L$ can be upper-bounded $a.e.$ as

$$\dot{V}_L \overset{a.e.}{\leqslant} \frac{1}{2}\|E_1\|^2 + \frac{1}{2}\|E_2\|^2 - \lambda_{\min}(\Lambda_1)\|E_1\|^2 - \lambda_{\min}(\Lambda_2)\|E_2\|^2 + \|R\|\rho(\|Z\|)\|Z\| - R^T (L_B \otimes I_m) K_s (L_B \otimes I_m) R - R^T (L_B \otimes I_m)^2 R. \tag{22}$$

Using the definition of the auxiliary gain constant Φ, which is positive given the sufficient gain conditions in (17) and the positive-definite property of L_B (note that the product $(L_B \otimes I_m)^2$ is positive-definite because L_B is positive-definite and symmetric), (22) is rewritten as

$$\dot{V}_L \overset{a.e.}{\leqslant} -\Phi\|Z\|^2 - \lambda_{\min}((L_B \otimes I_m) K_s (L_B \otimes I_m))\|R\|^2 + \|R\|\rho(\|Z\|)\|Z\|,$$

where the product $(L_B \otimes I_m) K_s (L_B \otimes I_m)$ is positive-definite because K_s is positive-definite and L_B is positive-definite and symmetric. After completing the squares, $\dot{V}_L$ is again upper-bounded $a.e.$ by

$$\dot{V}_L \overset{a.e.}{\leqslant} -\left(\Phi - \frac{\rho^2(\|Z\|)}{4\lambda_{\min}((L_B \otimes I_m) K_s (L_B \otimes I_m))}\right)\|Z\|^2.$$

Provided the gains $k_{s,i}$ are selected such that the respective minimum eigenvalues are sufficiently large such that $y(0) \in \mathcal{S}_{\mathcal{D}}$, there exists a constant $c \in \mathbb{R}_{>0}$ such that

$$\dot{V}_L \overset{a.e.}{\leqslant} -c\|Z\|^2 \tag{23}$$

for all $y \in \mathcal{D}$. Thus, the inequalities in (16) and (23) show that $V_L \in \mathcal{L}_\infty$ and, therefore, $E_1, E_2, R \in \mathcal{L}_\infty$. A simple analysis of the closed-loop error system shows that the remaining signals are also bounded. Furthermore, from (23), [32, Corollary 1] can be used to show $c\|Z\|^2 \to 0$ as $t \to \infty$ for all $y(0) \in \mathcal{S}_{\mathcal{D}}$. Because the vector Z contains the vector E_1, $\|E_1\| \to 0$ as $t \to \infty$. By Lemma 1, $\mathrm{d}(q_i, \mathrm{Conv}\{q_l \mid l \in \mathcal{V}_L\}) \to 0\ \forall i \in \mathcal{V}_F$, that is, each follower agent's state converges to the convex hull spanned by the leaders' states.

Note that the controller in (8) is distributed in communication; however, because the stabilizing set of initial conditions $\mathcal{S}_{\mathcal{D}}$ depends on the graph-dependent matrix L_B, the gains $k_{s,i}$ must be selected in a centralized manner before execution of the control. However, the set $\mathcal{S}_{\mathcal{D}}$ can be made arbitrarily large to include any initial condition $y(0)$ by increasing the minimum eigenvalues of the gains $k_{s,i}$ to increase the minimum eigenvalue of the matrix $(L_B \otimes I_m) K_s (L_B \otimes I_m)$. □

6. SIMULATION

To demonstrate the robustness of the developed approach in performing containment control of follower agents with respect to a set of leader agents, numerical simulations are performed for a group of AUVs conducting surveillance. Each follower agent is modeled as a conventional, slender-bodied,

[§]Because of the construction of $\boldsymbol{R}$ in (6), the set of time instances $\Theta \triangleq \{t \in \mathbb{R}_{\geqslant 0} \mid R^T (L_B \otimes I_m) \beta \mathcal{K}[\mathrm{Sgn}(E_2)] - R^T (L_B \otimes I_m) \beta \mathcal{K}[\mathrm{Sgn}(E_2)] \neq \{0\}\}$ can be represented by the union $\Theta = \cup_{k=1,\ldots,Fm} \Theta_k$, where $\Theta_k \triangleq \{t \in \mathbb{R}_{\geqslant 0} \mid E_{2_k} = 0 \wedge R_k \neq 0\}$. Because the signal $E_2 : \mathbb{R}_{\geqslant 0} \to \mathbb{R}^{Fm}$ is continuously differentiable, it can be shown that Θ_k is Lebesgue measure zero [28]. Because a finite union of Lebesgue measure zero sets is Lebesgue measure zero, Θ is Lebesgue measure zero. Hence, Θ is Lebesgue negligible.

DOI: 10.1002/rnc

fully actuated AUV with nonlinear dynamics as described in [33] (see [26] for more information on AUV dynamics). The state of each AUV is composed of surge (x), sway (y), heave (z), roll (ϕ), pitch (θ), and yaw (ψ). Actuation of the AUV is modeled by three independent forces acting at the center of mass of the vehicle and three independent moments, which can be produced with a given thruster configuration and an appropriate thruster mapping algorithm, such as that described in [34].

Four leader agents are used to direct five follower agents such that the follower agents' states converge to the convex hull formed by the leaders' time-varying states, which have initial positions shown in Table I, identical initial velocities of $[0.2\,\text{m/s}, 0\,\text{m/s}, 0.05\,\text{m/s}, 0\,\text{rad/s}, 0\,\text{rad/s}, -0.1\,\text{rad/s}]^T$, and identical accelerations of $[-0.02\sin(0.1t), -0.02\cos(0.1t), 0]^T$ m/s^2 in surge, sway, and heave, respectively, such that the leaders form an inclined rectangle that translates in a helical trajectory. The follower AUVs have initial positions shown in Table II and identical initial velocities of $[2\,\text{m/s}, 0\,\text{m/s}, 0\,\text{m/s}, 0\,\text{rad/s}, 0\,\text{rad/s}, 0\,\text{rad/s}]^T$. All leader and follower agents have initial roll, pitch, and yaw of 0 rad. The network topology is shown in Figure 1, where $a_{ij} = 1$ if $(j,i) \in \mathcal{E}_F \cup \mathcal{E}_L$ and $a_{ij} = 0$ otherwise. As in [35], the external disturbances for the follower AUVs are modeled as $[u_i \sin(0.5t), 0.5v_i \sin(0.25t)^{\dagger}, 0.2w_i\,\text{rand}]^T$ N in surge, sway, and heave, respectively, and 0 Nm in roll, pitch, and yaw, where $u_i, v_i, w_i \in \mathbb{R}$ represent the linear velocities in surge, sway, and heave, respectively, of the i^{th} follower agent and rand $\in \mathbb{R}_{[-1,1]}$ is a uniformly distributed random number generator. Identical gains for each follower agent i are selected as $k_{s,i} = \text{diag}(150, 150, 150, 1, 5, 70)$, $\chi_i = \text{diag}(50, 50, 50, 0.1, 0.2, 0.2)$, $\alpha_{1,i} = 0.2$, and $\alpha_{2,i} = 0.1$.

Table I. Leader initial positions in surge (x), sway (y), and heave (z).

Leader	x (m)	y (m)	z (m)
1	−0.5	0.5	0
2	−0.5	−0.5	0
3	0.5	−0.5	1‡
4	0.5	0.5	1‡

Table II. Follower initial positions in surge (x), sway (y), and heave (z).

Follower	x (m)	y (m)	z (m)
1	0	0.6	0.1
2	0.1	0.2	0.05
3	0.8	−0.2	0
4	−0.8	0.1	0.1
5	0.2	0.7	0.05

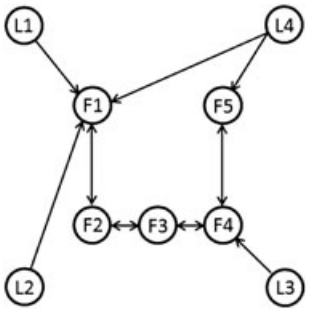

Figure 1. Network topology of leader ('L') and follower ('F') autonomous underwater vehicles.

†Correction added on 22 March 2016, after first online publication: "2.5" corrected to "0.25".
‡Correction added on 22 March 2016, after first online publication: "0" corrected to "1".

DOI: 10.1002/rnc

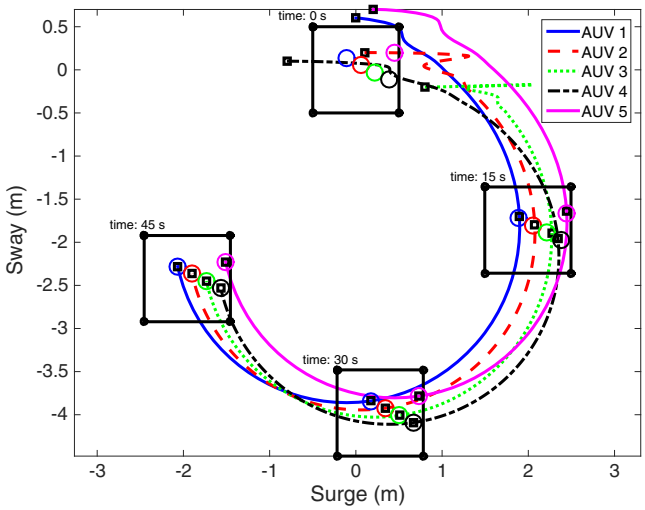

Figure 2. [Top view] Follower autonomous underwater vehicle trajectories in the surge (x) and sway (y) dimensions. At the labeled time instances, the black outline represents the projection of the leaders' convex hull onto surge and sway, black squares represent the follower positions, and circles within the leader outline represent the equilibrium trajectories of the followers.

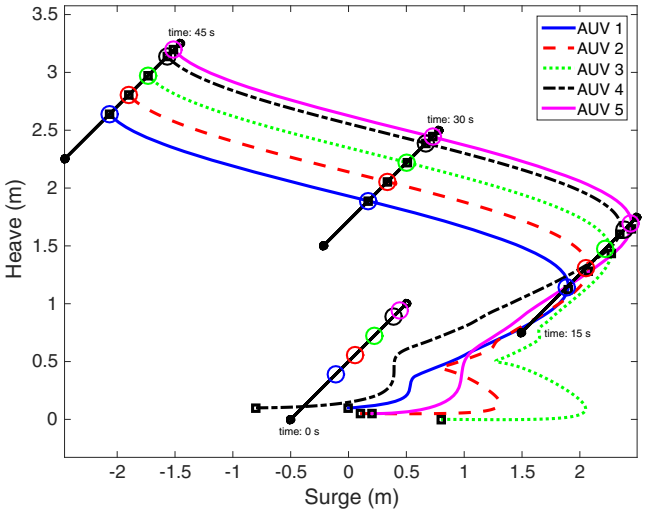

Figure 3. [Front view] Follower autonomous underwater vehicle trajectories in the surge (x) and heave (z) dimensions. At the labeled time instances, the black outline represents the projection of the leaders' convex hull onto surge and heave, black squares represent the follower positions, and circles within the leader outline represent the equilibrium trajectories of the followers.

The agents' trajectories are shown in Figures 2 and 3. At the labeled time instances, the black outline represents the projection of the leaders' convex hull onto the labeled dimensions, the black squares represent the follower agent positions, and the circles within the leader outline represent the equilibrium trajectories of the follower agents (which is a function of the network topology and leader trajectories, i.e., when $\|E_1\| \equiv 0$). The containment errors, that is, each dimension of the error signal $e_{1,i}$, are shown in Figure 4 for each agent, where $e_{1,i}^j$ indicates the j^{th} dimension of the vector $e_{1,i}$. In agreement with the analysis of the developed controller, Figures 2–4 indicate that the follower agents cooperatively become contained within the leader convex hull and converge to the containment equilibrium trajectories, despite the effects of model uncertainty and unknown time-varying exogenous disturbances. The Euclidean norms of the overall AUV force and moment actuation, shown in Figure 5, demonstrate that reasonable actuation levels are used.

DOI: 10.1002/rnc

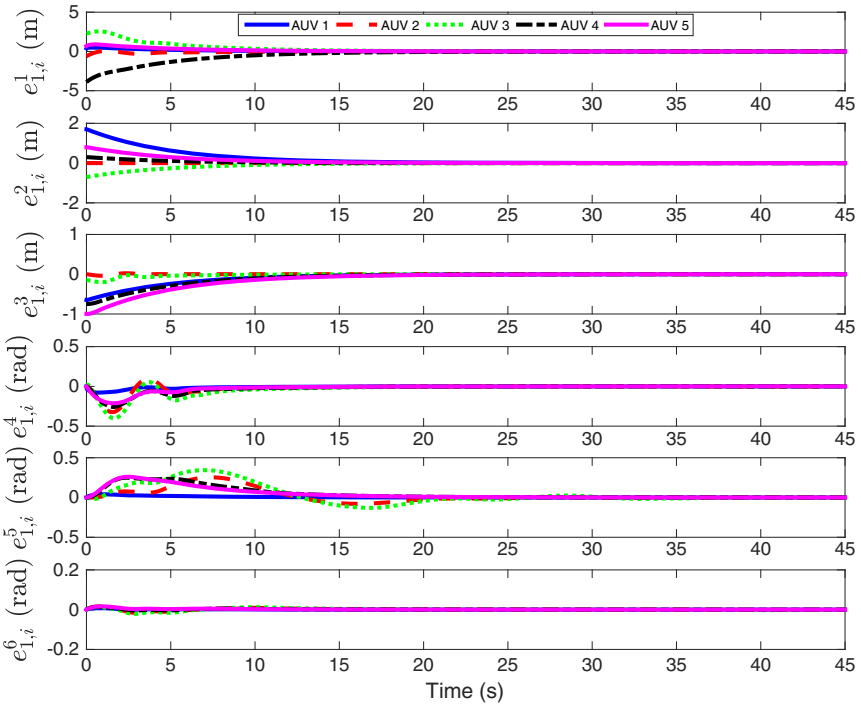

Figure 4. Containment errors of the follower autonomous underwater vehicles in surge, sway, heave, roll, pitch, and yaw.

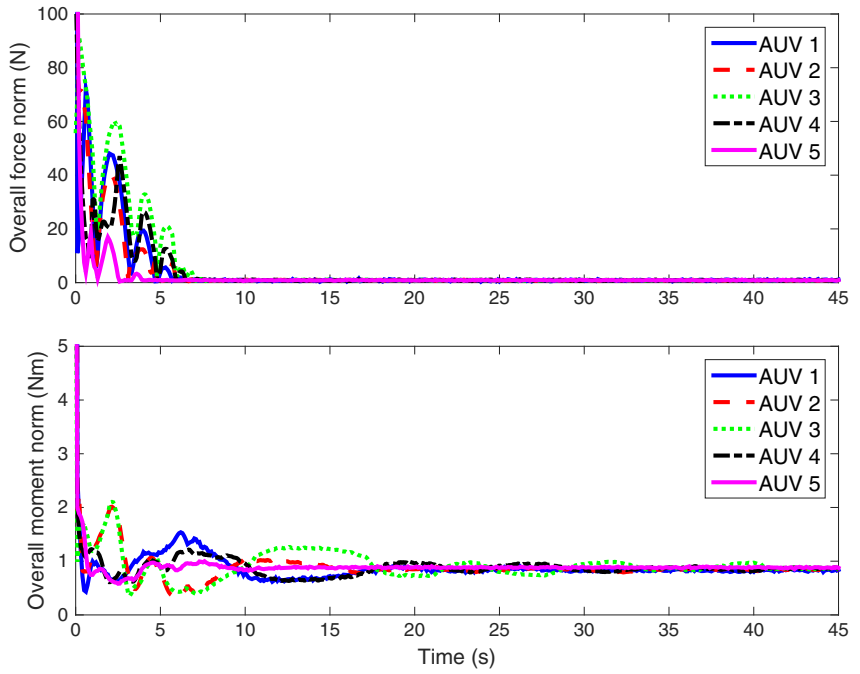

Figure 5. Euclidean norms of the follower autonomous underwater vehicle control efforts.

DOI: 10.1002/rnc

7. CONCLUSION

A distributed controller was developed for the cooperative containment control of autonomous networked follower agents with a set of network leaders, which is a generalization of the popular single leader–follower network. The developed continuous controller provides robustness to input disturbances and uncertain, nonlinear Euler–Lagrange dynamics such that the state of each follower agent asymptotically converges to the convex hull spanned by the leaders' time-varying states for an arbitrary number of leaders. Some notable assumptions are that the agents' dynamics and disturbances are smooth, the graph containing the follower agents is connected, and at least one follower agent is connected to at least one leader. Simulation results are provided to demonstrate the disturbance rejection capability of the developed controller. Future work may include extension of the given stability analysis to show stability of the networked system when using the controller in (8) for a general digraph, such as in [18]; the limitation of the current analysis is that it requires the matrix L_B to be positive-definite, which is not necessarily the case for a follower agent network topology that is directed. Future research on cooperative containment control may also include the development of a distributed controller that is subject to the effects of practical communication, such as communication delays and packet dropouts (cf. [36–39]).

APPENDIX

Proof of Lemma 1

Because the eigenvalues of L_B are positive by Assumptions 5 and [9, Lemma 4.1], the diagonal entries are positive, and the off-diagonal entries are nonpositive, all entries of the matrix L_B^{-1} are nonnegative [40, Theorem 2.3]. Because of the structure of the Laplacian matrix $\mathcal{L}$, we have that $\mathcal{L}\mathbf{1}_{F+L} = \mathbf{0}_{F+L}$, which implies $L_B\mathbf{1}_F + \mathcal{L}_L\mathbf{1}_L = \mathbf{0}_L$, where $\mathbf{1}$ is a column vector of ones with the denoted dimension. Because L_B is invertible, $\mathbf{1}_F = -L_B^{-1}\mathcal{L}_L\mathbf{1}_L$, which implies that row sums of $-L_B^{-1}\mathcal{L}_L$ add to one, where each entry of the matrix $-L_B^{-1}\mathcal{L}_L$ is nonnegative because L_B^{-1} has only nonnegative entries and $\mathcal{L}_L$ has only nonpositive entries. Thus, the product $-\left(\left(L_B^{-1}\mathcal{L}_L\right)\otimes I_m\right)Q_L$ can be represented as $\left[\, q_{d1}^T,\, \ldots,\, q_{dF}^T \,\right]^T = -\left(\left(L_B^{-1}\mathcal{L}_L\right)\otimes I_m\right)Q_L \in \mathbb{R}^{Fm}$, where $q_{di} \in \mathbb{R}^m$ such that $q_{di} = \sum_{l\in\{1,\ldots,L\}}\left[-L_B^{-1}\mathcal{L}_L\right]_{il} q_l \;\forall i \in \{1,\ldots,F\}$, where $[\cdot]_{ij}$ denotes the matrix entry of the i^{th} row and j^{th} column, $\sum_{l\in\{1,\ldots,L\}}\left[-L_B^{-1}\mathcal{L}_L\right]_{il} = 1$ $\forall i \in \{1,\ldots,F\}$, and $\left[-L_B^{-1}\mathcal{L}_L\right]_{il} \geqslant 0 \;\forall i \in \{1,\ldots,F\}, \forall l \in \{1,\ldots,L\}$ by the aforementioned conclusions. Because the convex hull for the set $S \triangleq \{q_l \mid l \in \mathcal{V}_L\}$ is defined as $\text{Conv}\{S\} \triangleq \left\{\sum_{l\in\mathcal{V}_L}\alpha_l q_l \mid (\forall l : \mathbb{R} \ni \alpha_l \geqslant 0) \wedge \sum_{l\in\mathcal{V}_L}\alpha_l = 1\right\}$ [41], we have that $q_{di} \in \text{Conv}\{q_l \mid l \in \mathcal{V}_L\}$ $\forall i \in \{1,\ldots,F\}$; in other words, the vectors stacked in the product $-\left(\left(L_B^{-1}\mathcal{L}_L\right)\otimes I_m\right)Q_L$ are within the convex hull formed with the leader agents' states. Suppose that $\|E_1\| \to 0$. Then $\left\|\left(L_B\otimes I_m\right)^{-1}E_1\right\| \to 0$, which implies that $\left\|Q_F + \left(\left(L_B^{-1}\mathcal{L}_L\right)\otimes I_m\right)Q_L\right\| \to 0$ by (4), and thus, $Q_F = \left[\, q_{L+1}^T,\, \ldots,\, q_{L+F}^T \,\right]^T \to -\left(\left(L_B^{-1}\mathcal{L}_L\right)\otimes I_m\right)Q_L = \left[\, q_{d1}^T,\, \ldots,\, q_{dF}^T \,\right]^T$. Hence, $\text{d}\left(q_i, \text{Conv}\{q_l \mid l \in \mathcal{V}_L\}\right) \to 0 \;\forall i \in \mathcal{V}_F$. □

ACKNOWLEDGEMENT

The authors would like to thank the AFRL Mathematical Modeling and Optimization Institute and NSF, contract/grant numbers 1161260 and 1217908, for the financial support.

REFERENCES

1. Olfati-Saber R, Fax JA, Murray RM. Consensus and cooperation in networked multi-agent systems. *Proceedings of the IEEE* 2007; **95**(1):215 –233.
2. Ren W, Beard RW, Atkins EM. Information consensus in multivehicle cooperative control. *IEEE Control Systems Magazine* 2007; **27**:71–82.
3. Ren W, Beard RW. *Distributed Consensus in Multi-vehicle Cooperative Control*. Springer-Verlag: New York, 2008.

DOI: 10.1002/rnc

4. Kan Z, Klotz J, Cheng TH, Dixon WE. Ensuring network connectivity for nonholonomic robots during decentralized rendezvous. *Proceedings of the American Control Conference*, Montreal, Canada, 2012; 3718–3723.
5. Rodriguez-Angeles A, Nijmeijer H. Mutual synchronization of robots via estimated state feedback: a cooperative approach. *IEEE Transactions on Control Systems Technology* 2004; **12**(4):542–554.
6. Ren W. Multi-vehicle consensus with a time-varying reference state. *Systems & Control Letters* 2007; **56**:474–483.
7. Nuño E, Ortega R, Basañez L, Hill D. Synchronization of networks of nonidentical Euler–Lagrange systems with uncertian parameters and communication delays. *IEEE Transactions on Automatic Control* 2011; **56**(4):935–941.
8. Klotz JR, Kan Z, Shea JM, Pasiliao EL, Dixon WE. Asymptotic synchronization of a leader–follower network of uncertain Euler–Lagrange systems. *IEEE Transactions on Control Network Systems* 2014; **2**(2):174–182.
9. Notarstefano G, Egerstedt M, Haque M. Containment in leader–follower networks with switching communication topologies. *Automatica* 2011; **47**(5):1035–1040.
10. Dimarogonas DV, Tsiotras P, Kyriakopoulos KJ. Leader–follower cooperative attitude control of multiple rigid bodies. *Systems & Control Letters* 2009; **58**:429–435.
11. Mei J, Ren W, Chen J, Ma G. Distributed adaptive coordination for multiple Lagrangian systems under a directed graph without using neighbors' velocity information. *Automatica* 2013; **49**(6):1723–1731.
12. Ji M, Ferrari-Trecate G, Egerstedt M, Buffa A. Containment control in mobile networks. *IEEE Transactions on Automatic Control* 2008; **53**(8):1972–1975.
13. Cao Y, Stuart D, Ren W, Meng Z. Distributed containment control for multiple autonomous vehicles with double-integrator dynamics: algorithms and experiments. *IEEE Transactions on Control Systems Technology* 2011; **19**(4):929–938.
14. Li J, Ren W, Xu S. Distributed containment control with multiple dynamic leaders for double-integrator dynamics using only position measurements. *IEEE Transactions on Automatic Control* 2012; **57**(6):1553–1559.
15. Cao Y, Ren W, Egerstedt M. Distributed containment control with multiple stationary or dynamic leaders in fixed and switching directed networks. *Automatica* 2012; **48**:1586–1597.
16. Kan Z, Klotz J, Pasiliao EL, Dixon WE. Containment control for a directed social network with state-dependent connectivity. *Proceedings of the American Control Conference*, Washington DC, 2013; 1953–1958.
17. Meng Z, Ren W, You Z. Distributed finite-time attitude containment control for multiple rigid bodies. *Automatica* 2010; **46**(12):2092–2099.
18. Mei J, Ren W, Ma G. Distributed containment control for Lagrangian networks with parametric uncertainties under a directed graph. *Automatica* 2012; **48**(4):653–659.
19. Dong X, Meng F, Shi Z, Lu G, Zhong Y. Output containment control for swarm systems with general linear dynamics: a dynamic output feedback approach. *Systems & Control Letters* 2014; **71**:31–37.
20. Yang D, Ren W, Liu X. Fully distributed adaptive sliding-mode controller design for containment control of multiple Lagrangian systems. *Systems & Control Letters* 2014; **72**:44–52.
21. Ortega R, Loría A, Nicklasson PJ, Sira-Ramirez HJ. *Passivity-based Control of Euler–Lagrange Systems: Mechanical, Electrical and Electromechanical Applications*. Springer-Verlag: London, 1998.
22. Mehrabian AR, Khorasani K. Cooperative optimal synchronization of networked uncertain nonlinear Euler–Lagrange heterogeneous multi-agent systems with switching topologies. *Journal of Dynamical Systems, Measurement, Control* 2015; **137**(4):12 pages.
23. Nuño E, Ortega R, Jayawardhana B, Basañez L. Coordination of multi-agent Euler–Lagrange systems via energy-shaping: networking improves robustness. *Automatica* 2013; **49**(10):3065–3071.
24. Liu YC, Chopra N. Synchronization of networked mechanical systems with communication delays and human input. *ASME Journal of Dynamical Systems, Measurement, and Control* 2013; **135**(4):041004.
25. Makkar C, Hu G, Sawyer WG, Dixon WE. Lyapunov-based tracking control in the presence of uncertain nonlinear parameterizable friction. *IEEE Transactions on Automatic Control* 2007; **52**:1988–1994.
26. Fossen TI. *Handbook of Marine Craft Hydrodynamics and Motion Control*. Wiley, 2011.
27. Patre P, Mackunis W, Dupree K, Dixon WE. Modular adaptive control of uncertain Euler–Lagrange systems with additive disturbances. *IEEE Transactions on Automatic Control* 2011; **56**(1):155–160.
28. Kamalapurkar R, Rosenfeld JA, Klotz J, Downey RJ, Dixon WE. *Supporting lemmas for RISE-based control methods*, 2014. arXiv:1306.3432v3.
29. Chopra N, Stipanović DM, Spong MW. On synchronization and collision avoidance for mechanical systems. *Proceedings of the American Control Conference*, Seattle, WA, 2008; 3713–3718.
30. Paden BE, Sastry SS. A calculus for computing Filippov's differential inclusion with application to the variable structure control of robot manipulators. *IEEE Transactions on Circuits and Systems* 1987; **34**(1):73–82.
31. Shevitz D, Paden B. Lyapunov stability theory of nonsmooth systems. *IEEE Transactions on Automatic Control* 1994; **39**(9):1910–1914.
32. Fischer N, Kamalapurkar R, Dixon WE. Lasalle–Yoshizawa corollaries for nonsmooth systems. *IEEE Transactions on Automatic Control* 2013; **58**(9):2333–2338.
33. Prestero T. Verification of a six-degree of freedom simulation model for the REMUS autonomous underwater vehicle. *Master's Thesis*, University of California at Davis, 1994.
34. Hanai A, Choi HT, Choi SK, Yuh J. Experimental study on fine motion control of underwater robots. *Advanced Robotics* 2004; **18**(10):963–978.
35. Fischer N, Bhasin S, Dixon WE. Nonlinear control of an autonomous underwater vehicle: a RISE-based approach. *Proceedings of the American Control Conference* 2011:3972–3977.

DOI: 10.1002/rnc

36. Guo G, Lu Z, Han QL. Control with Markov sensors/actuators assignment. *Transactions on Automatic Control* 2012; **57**(7):1799–1804.
37. Ding L, Han QL, Guo G. Network-based leader-following consensus for distributed multi-agent systems. *Automatica* 2013; **49**(7):2281–2286.
38. Guo G, Ding L, Han QL. A distributed event-triggered transmission strategy for sampled-data consensus of multi-agent systems. *Automatica* 2014; **50**(5):1489–1496.
39. Klotz JR, Obuz S, Kan Z, Dixon WE. Synchronization of uncertain Euler–Lagrange systems with unknown time-varying communication delays. *Proceedings of the American Control Conference*, Chicago, IL, 2015; 683–688.
40. Berman A, Plemmons RJ. *Nonnegative Matrices in the Mathematical Sciences*, Computer Science and Applied Mathematics. Academic Press: New York, New York, 1979.
41. Boyd S, Vandenberghe L. *Convex Optimization*. Cambridge University Press: New York, NY USA, 2004.

DOI: 10.1002/rnc